

Temperature effect and stress on microcrystalline silicon thin films deposited under high pressure plasma conditions

E. Amanatides^a, E. Katsia^a, D. Mataras^{a,*}, A. Soto^b, G.A. Voyiatzis^b

^a Plasma Technology Laboratory, Department of Chemical Engineering, University of Patras, P.O. Box 1407, 26504 Patras, Greece

^b FORTH/ICE-HT, P.O. Box 1414, 26504 Patras, Greece

Available online 18 January 2006

Abstract

An investigation of the effect of the deposition pressure (133.3–1333 Pa) on the $\mu\text{c-Si:H}$ crystallinity, stress and thermal stability was performed. The films were deposited from SiH_4/H_2 discharges under constant power conditions and with constant silane partial pressure. The increase of pressure resulted in an optimum of the deposition rate at 333.3 Pa and an increase of the crystallinity as the pressure is raised from 133.3 to 333.3 Pa. The Raman spectra revealed a shift of the c-Si peak for all films towards lower wave numbers and this shift was much larger for the film deposited at 133.3 Pa. The effect of film stress and local heating in this shift was distinguished by investigating the effect of temperature on the position of the c-Si peak. The stress of the deposited films was found to be tensile for all pressures and much higher for the film deposited at 133.3 Pa. This result is discussed in terms of the deposition conditions pointing out the advantages of working at higher pressures.

© 2005 Elsevier B.V. All rights reserved.

Keywords: Microcrystalline silicon; Amorphous silicon; Film stress; Raman spectroscopy

1. Introduction

Recently, micro- and nano-crystalline silicon thin films produced by low temperature plasma processes have found application in various devices including thin film solar cells, light sensors and thin film transistors. The performance of these devices is a function of the electronic and optical properties of the material that in turn critically depends on its structural properties. Thus, crystalline volume fraction [1], crystallite size [2], residual stress [3] and hydrogen bonding [4] are important characteristics that require careful determination and optimization.

Among the techniques typically used for the structural characterization of silicon thin films, Laser Raman spectroscopy is recognized as the most powerful one because it can provide information on almost all of the above mentioned properties. However, the analysis of Raman spectra and the calculation of the specific film properties require special attention due to the possible coexistence of various effects that impose difficulties in their interpretation. Such phenomena

are: a) Laser induced crystallization [5] b) shift of the peaks' frequency due to local heating and lattice anharmonicity [6] c) shift of the peaks' frequency due to tensile or compressive stress [7] and d) shift of the peaks' frequency due to the reduction of the size of the crystallites [8].

Taking into account the above mentioned difficulties, the present work presents an effort to apply laser Raman spectroscopy for the investigation of the thermal stability and stress of microcrystalline silicon thin films deposited from SiH_4/H_2 discharges, at different gas pressures (133.3 to 1333 Pa). High pressure conditions have been preferred as this region has attracted particular attention recently, due to the possibility to prepare device quality thin films at relatively high growth rates [9,10]. The depositions were performed in conditions of constant power consumption in the discharge and for constant silane partial pressure in order to isolate the effect of the total gas pressure on the film stress and stability, as much as possible. The Raman spectra of these films were excited by the 441.6 nm line of a HeCd laser and by the 514.5 nm line of an air-cooled Ar^+ laser. The increase of the film temperature was induced by increasing the laser power and simultaneously recording the excited Raman spectra. The temperature effect was then distinguished from the Raman spectra thus allowing the determination of the film stress.

* Corresponding author. Tel.: +30 261 0997857; fax: +30 261 0993361.

E-mail address: dim@plasmatech.gr (D. Mataras).

Significant differences were found in thin films deposited at different pressures concerning either the film stress or the heating resistance.

2. Experimental

The depositions of $\mu\text{c-Si:H}$ films were carried out in a capacitively coupled Ultra High Vacuum parallel plate reactor having a base vacuum of 10^{-9} mbar. The 120 mm in diameter RF electrode is fixed to the chamber while the 90 mm grounded deposition electrode can be moved to vary the interelectrode spacing. All the experiments were performed using an excitation frequency of 13.56 MHz and a constant electrode gap of 15 mm. Constant thickness (2 μm) films were deposited on Corning 7059 at a substrate temperature of 250 °C using electronic quality gases.

The amount of RF power actually fed into the discharge chamber was determined using an accurate method employing the Fourier transform determination of power and phase from current and voltage measurements [11]. Many sets of electrical measurements were initially performed to determine the RF voltages leading to constant RF power dissipation in the discharge for the entire range of pressures. The set of voltages leading to a constant power of 72 mW/cm^2 (8W in total) was chosen from those sets to ensure a capacitive regime and to avoid powder formation at higher pressures. In addition, Laser Reflectance Interferometry has been used for the in situ monitoring of the deposition rate [12].

In any case, powder suppression techniques were used together with laser light scattering measurements to ensure dust-free conditions. Namely, in this series of experiments, relatively high flow rates (400 sccm) were maintained while using a low silane partial pressure. Furthermore, the constant 3.33 Pa silane partial pressure was achieved by decreasing the flow rate of silane with increasing pressure, using mass flow controllers. A downstream throttle valve controller was used to adjust independently the total working pressure.

Raman spectra excited by the 514.5 nm line of an air-cooled Ar^+ laser (Spectra Physics), were measured with the T-64000 Raman system (J.Y.) in the triple subtractive configuration. A proper interference filter was used to reject plasma lines. The excitation beam was directed towards the microscope and with the use of a beam splitter and a Long Working distance microscope objective (50 \times /0.55 Olympus) it was focused onto the sample. The spectra were obtained using a 1 mW laser power on the specimen for a total integration time of 200 s. Raman scattered radiation was collected in back-scattering geometry by the same microscope objective and passing through the beam splitter and was focused on the slit of a pre-monochromator. The dispersion and the detection were done by an 1800-grooves/mm grating and by a 2D CCD detector (operating at 140 K), respectively.

Raman spectra, excited with the 441.6 nm line of an air-cooled HeCd laser (Kimmon Electric Co.), were measured with the UV-Vis Labram HR-800 spectrograph (J.Y.). A narrow-bandpass interference filter was used for the elimination of the laser plasma lines. The excitation beam was directed to the

sample compartment of a confocal open microscope attachment for punctual analysis. The microscope was used for the delivery of the excitation laser beam on the sample and the collection of the back-scattered light through a notch-filter and the objective lens adapted to the aperture of the microscope. The focusing objective was a Long Working distance (8 mm) 50 \times /0.55 Olympus lens, as well. The spectra were obtained using a 3.5 mW laser power on the specimen for a total integration time of 200 s. The Raman scattered radiation was focused on a confocal entrance slit (200 μm width) of an achromatic flat field spectrograph with 800 nm focal length. A 1800-grooves/mm grating and a 2D CCD detector (operating at 140 K) did the dispersion and the detection of the Raman photons, respectively.

3. Results and discussion

The depositions of $\mu\text{c-Si:H}$ thin films were performed from SiH_4/H_2 discharges, under constant power conditions (72 mW/cm^2) and for constant silane partial pressure. Experimentally, the constant silane partial pressure (3.33 Pa) was achieved by reducing the fraction of SiH_4 in H_2 from 2.5% to 0.25% as the total pressure was increased, with a step of 333.3 Pa, from 133.3 to 1333 Pa. On the other hand, constant power consumption in the discharge (8 Watt/72 mW/cm^2) was achieved by adjusting the RF voltage while performing voltage and current waveform measurements as described in the Experimental section. Fig. 1 (left axis) shows the variation of the deposition rate as a function of the total gas pressure. The increase of pressure leads to a maximum deposition rate for the pressure of 333.3 Pa. An increase beyond this pressure results in a drop of the deposition rate to about 1 $\text{\AA}/\text{sec}$ at 1333 Pa. The existence of this optimum was thoroughly discussed in a previous work of this group [13] and was related to the pressure where the SiH_4 dissociation rate to free radicals is rather high, while the fluxes of species to the surfaces are not significantly hindered and the secondary gas phase reactions are mainly a source of additional film precursors.

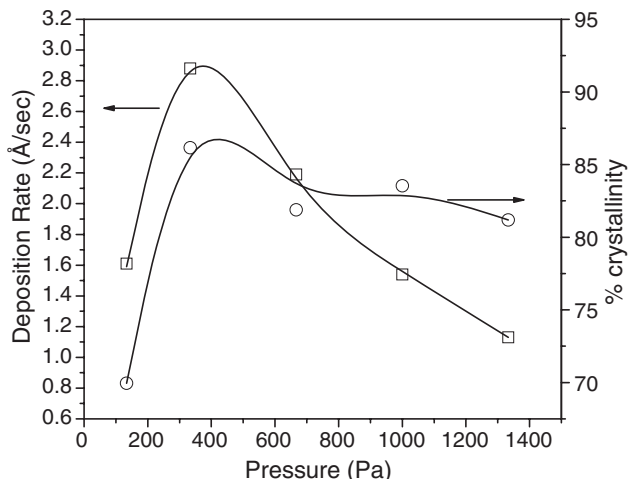


Fig. 1. Deposition rate (left axis) and percentage of film crystallinity (right axis) as functions of the total gas pressure.

In addition, Fig. 1 (right axis) presents the variation of the thin film crystallinity as a function of the total gas pressure. The crystallinity increases as we go from 133.3 to 333.3 Pa and then is almost unaffected by a further increase of pressure. It is also remarkable to note that the highest crystallinity is observed at 333.3 Pa where the deposition rate is maximized. The method used for calculating the crystallinity was presented in Ref. [14] and it is based on the deconvolution of the Raman spectra in 3 peaks, one between 516 and 521 cm^{-1} depending on the spectra (c-Si), one at 480 cm^{-1} (a-Si) and one at 501 cm^{-1} (grain boundaries—grains with diameter $<30 \text{ \AA}$). Lorentzian peaks were used for the fitting of the Raman spectra and the fitting results were very good in the case of 3 peaks deconvolution. Other methods, as two peaks deconvolution and the subtraction of an a-Si:H spectra, were also tried but the fitting results were always worst.

The calculation of the percentage of film crystallinity was based on the recorded Raman spectra of the films that are shown in Fig. 2. These spectra were excited by the 514.5 nm line of an air-cooled Ar^+ laser with a power of 1 mW on the specimen. The entire set exhibits the characteristic peak of c-Si, located around 521 cm^{-1} , identifying the microcrystalline character of the films. A low-frequency shoulder of this peak shifted to lower wave numbers is also present in all the spectra and corresponds to the amorphous phase. Fig. 2 includes also the spectra of a c-Si wafer used as a reference for monitoring the c-Si peak shift. As we can observe all films show a slight shift of the c-Si peak towards lower wave numbers. The highest displacement of the c-Si peak is observed for the film deposited at 133.3 Pa ($\sim 517 \text{ cm}^{-1}$). This, as already discussed in the introduction, can be attributed to either a tensile stress of $\mu\text{c-Si:H}$ or to local heating due to the laser power or to a reduction of the crystallites' size. The latter can be excluded in our case, where the crystallinity is rather high and the deposition conditions are quite far from either the transition to amorphous silicon or to extremely high dilution of SiH_4 in H_2 . However,

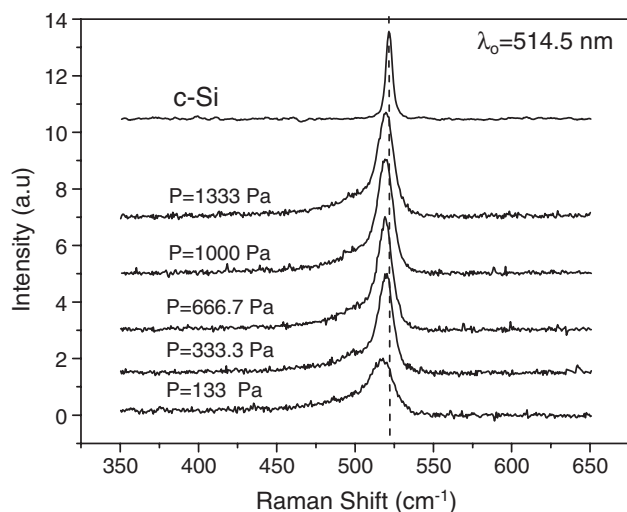


Fig. 2. Raman spectra from 350 to 650 cm^{-1} of $\mu\text{c-Si:H}$ thin films deposited at different pressures and of c-Si used as a reference for the peak shift.

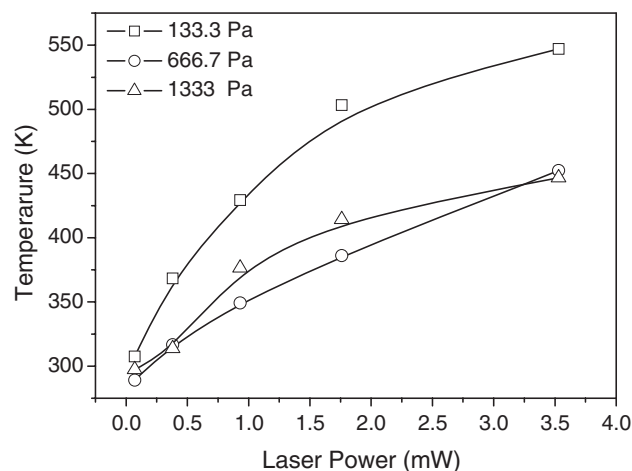


Fig. 3. Film temperature measured from Stokes and anti-Stokes lines as a function of the laser power for films deposited at 133.3, 333.3 and 1333 Pa.

the peak shift cannot be definitely attributed to either film stress or the temperature effect due to laser heating.

Thus, in order to clarify the origin of the peak shift, the effect of temperature on the Raman spectra of the specific films was investigated. The increase of the film temperature was induced by altering the laser power from 0.07 to 3.5 mW. For this study, the 441.6 nm line of a HeCd laser was used, as the demanding variation of the Ar^+ laser power was not possible. It is also worth noting that the power of 0.07 mW is the lowest power, where a meaningful Raman signal can be obtained. The film temperature that was developed due to the power increase was calculated from the integrated ratio of Stokes to anti-Stokes peaks [15]. Fig. 3 presents the variation of the film temperature as a function of the laser power for the films deposited at 133.3, 333.3 and 1333 Pa. The increase of laser power leads to a rise of the film temperature for all materials which still remains below the deposition temperature. However, the temperature developed for the same laser power was always lower for the films prepared at pressures of 333.3 and 1333 Pa compared to the film deposited at 133.3 Pa. This indicates higher heat conduction in these films, which in turn reveals that denser films are deposited at higher pressures.

Furthermore, in order to review the effect of temperature on the shift of the c-Si peak, Fig. 4 presents the Raman spectra obtained at different film temperatures for the film deposited at 1333 Pa. As we can observe, the increase of temperature results in a continuous displacement of the c-Si peak to lower wave numbers. This shift has been the subject of several theoretical and experimental works that can be found in the literature for c-Si, a-Si:H and $\mu\text{c-Si:H}$ [8]. It is attributed to the anharmonicity of the lattice forces and the vibrational potential energy. According to the anharmonicity degree that is used, different expressions can be found that relate the peak shift and the full width at half maximum (FWHM) with the temperature and a review of such relations can be found in Ref. [8]. In our case and for the film deposited at 1333 Pa, the peak shift starts for a film temperature higher than 350 K, below this temperature no shift due to heating was observed. It is also worth noting that

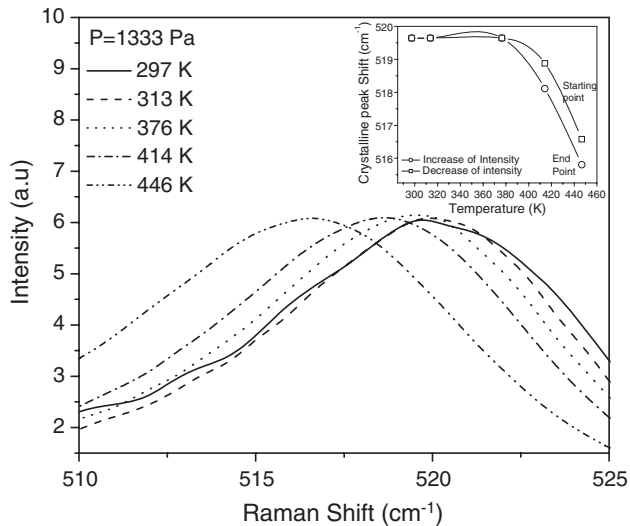


Fig. 4. Raman spectra from 510 to 525 cm^{-1} of the film deposited at 1333 Pa for different film temperatures. The inset figure shows the variation of the peak position as a function of the deposition temperature, measured when first increasing and then decreasing the laser power.

the effect of temperature on the peak shift is reversible. This is presented in the inset of Fig. 4, where the peak shift is plotted as a function of the induced temperature when first increasing and then decreasing the laser power. Despite the small differences observed, especially at higher temperatures, the peak shift is about the same either if one increases or decreases the film temperature, indicating that the variation of temperature cannot produce permanent microstructural changes, at least in this range.

Fig. 5 summarizes the results concerning the effect of temperature on both the peak shift (left axis) and FWHM (right axis) for the films deposited at 133.3, 333.3 and 1333 Pa. It can be observed that the increase from room temperature up to 350 K affects only slightly the c-Si peak position and the FWHM of all the films. Further increase of temperature up to 450 K leads to a displacement of the c-Si peak of about 3 cm^{-1} and an increase of the FWHM of about 1 cm^{-1} for all films. Finally, the increase of the film temperature (only for the 133.3 Pa

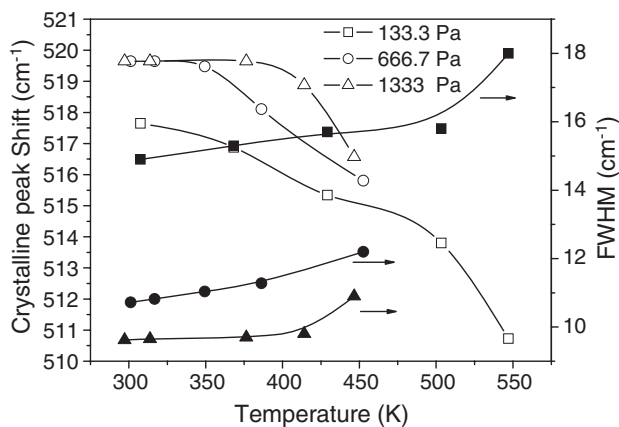


Fig. 5. Variation of the c-Si peak position (left axis) and of the FWHM (right axis) as a function of temperature for the films deposited at 133.3, 333.3 and 1333 Pa.

Table 1

The c-Si peak shift according to the spectra obtained at room temperature for 514.5 and 441.6 nm excitation and the value of tensile stress calculated from the peak shift of the films deposited at different pressures

Pressure (Pa)	$\Delta\omega$ (cm^{-1}) 514.5 nm	$\Delta\omega$ (cm^{-1}) 441.6 nm	σ (MPa)
133.3	4.2	4.1	1035
333.3	1.7	2.1	475
666.5	2.3	–	587.5
1000	2.1	–	525
1333	1.9	2.1	500

sample) up to 550 K leads to an abrupt increase of both the peak shift and the FWHM. It is quite clear through these observations that the effect of temperature on the peak position and the FWHM is nearly independent of the films, at least in our case where the percentage of crystalline volume fraction of all films is high. It is also worth mentioning that as in the case of 514.5 nm excitation (Fig. 2), the spectra obtained with the 441.6 nm line give at room temperature a crystalline silicon peak located at $\sim 520 \text{ cm}^{-1}$ for the films deposited at 333.3 and 1333 Pa and at $\sim 517 \text{ cm}^{-1}$ for the film deposited at 133.3 Pa. This agreement in combination with the results concerning the temperature effect on the peak shift, allow us to attribute the peak shift at room temperature to the stress of the deposited films.

Table 1 summarizes the c-Si peak shift ($\Delta\omega$) for the spectra obtained at room temperature and for both excitations (514 and 441.6 cm^{-1}) and the stress as calculated according to the formula [16]:

$$\sigma(\text{MPa}) = -250\Delta\omega \quad (1)$$

which indicates that all films present tensile stresses. In addition, the film deposited at 133.3 Pa presents the highest stress, while the films deposited above 333.3 Pa present slight differences. This behavior can also be explained by taking into account the deposition conditions. Namely, at 133.3 Pa, the H_2 density and consequently the H atoms density and flux are expected to be lower compared to all other pressures. In addition, at 133.3 Pa the ions reaching the growing film surface may have enough energy to disrupt the crystallite structure. Both the lower H atoms flux and the higher ion energy can explain the higher stress and the lower crystallinity at this pressure. On the other hand, at higher pressures, although in some cases (333.3 Pa) the deposition rate is faster compared to 133.3 Pa, the significant increase of H_2 density seems to be enough for releasing the stress from the depositing films and for maintaining higher crystalline volume fraction. Whatever is the case, the much lower stress that was predicted for the films deposited at higher pressures may be taken as another important advantage of working in the high pressure regime.

4. Conclusions

An investigation of the effect of the total gas pressure (133.3–1333 Pa) on the $\mu\text{c-Si:H}$ thin film percentage of crystallinity, stress and thermal stability was performed. The films were deposited under constant power consumption in

SiH₄/H₂ discharges and with a constant SiH₄ partial pressure, in order to isolate the effect of the total gas pressure as much as possible.

The increase of pressure has led to a clear optimum of the deposition rate at 333.3 Pa, while at the same time the crystallinity of the films was favored by the pressure increase from 133.3 to 333.3 Pa, remaining almost unaffected above this pressure.

Moreover, the Raman spectra have shown a c-Si peak shift for all films which was much stronger for the film deposited at 133.3 Pa. The contribution of stress and local heating on the observed shift was distinguished by investigating the effect of temperature on the peak shift and on the FWHM. The film deposited at 133.3 Pa was much more sensitive to exposure at different laser powers indicating lower heat conduction and less dense films at this condition.

The effect of temperature on the peak shift and FWHM was almost independent of the films that were studied and almost negligible at room temperature. This allowed the calculation of the film stress that was found to be tensile for all films and it was much higher for the film deposited at 133.3 Pa compared to all other pressures, indicating another important advantage of working at higher pressures.

Acknowledgments

Two of the authors (E. Amanatides and D. Mataras) wish to thank the European Social Fund (ESF) Operational Program for Educational and Vocational Training II EPEAEK II, and

particularly the Program PYTHAGORAS for funding this work.

References

- [1] O. Vetterl, F. Finger, R. Carius, P. Hapke, L. Houben, O. Kluth, A. Lambertz, A. Muck, B. Rweh, H. Wagner, *Sol. Energy Mater. Sol. Cells* 62 (2000) 97.
- [2] H. Tuir, J. Dixmier, K. Zellama, J.-F. Morhange, P. Elkaim, *J. Non-Cryst. Solids* 227–230 (1998) 906.
- [3] Y. Gogotsi, C. Baek, F. Kirscht, *Semicond. Sci. Technol.* 14 (1999) 936.
- [4] S. Vingoli, R. Butte, R. Meaudre, M. Meaudre, R. Brenier, *J. Phys., Condens. Matter* 15 (2003) 7185.
- [5] S.B. Concari, R.H. Buitrago, *Semicond. Sci. Technol.* 18 (2003) 864.
- [6] R. Tsu, J.G. Hernandez, *Appl. Phys. Lett.* 41 (1982) 1016.
- [7] V. Paillard, P. Puech, R. Sirvin, S. Hamma, P. Roca i Cabarrocas, *J. Appl. Phys.* 90 (2001) 3276.
- [8] G. Viera, S. Huet, L. Boufendi, *J. Appl. Phys.* 90 (2001) 3276.
- [9] T. Roschek, T. Repmann, J. Müller, B. Rech, H. Wagner, *J. Vac. Sci. Technol., A* 20 (2002) 492.
- [10] M. Kondo, M. Fukawa, L. Guo, A. Matsuda, *J. Non-Cryst. Solids* 266–269 (2000) 84.
- [11] N. Spiliopoulos, D. Mataras, D.E. Rapakoulis, *J. Vac. Sci. Technol., A* 14 (1996) 2757.
- [12] E. Amanatides, S. Stamou, S. Boghosian, D. Mataras, *Proceedings of the 16th European Photovoltaic Solar Energy Conference, Glasgow, UK, vol. 1, 2000*, p. 581.
- [13] E. Amanatides, A. Hammad, E. Katsia, D. Mataras, *J. Appl. Phys.* 97 (2005) 073303.
- [14] E. Katsia, E. Amanatides, D. Mataras, A. Soto, G.A. Voyiatzis, *Sol. Energy Mater. Sol. Cells* 87 (2005) 157.
- [15] M.F. Cerqueira, J.A. Ferreira, *J. Mater. Process. Technol.* 92–93 (1999) 235.
- [16] I. De Wolf, *Semicond. Sci. Technol.* 11 (1996) 139.